Desalination and Water Treatment
www.deswater.com

doi: 10.5004/dwt.2019.23348

137 (2019) 312–327
January

Heterogeneous photocatalytic degradation and mineralization of 2,4-dichlorophenoxy acetic acid (2,4-D): its performance, kinetics, and economic analysis

Gamze Dogdu Okcu[a], Hatice Eser Okten[b], Arda Yalcuk[a,*]

[a]*Department of Environmental Engineering, Abant Izzet Baysal University, 14030 Golkoy Campus, Bolu, Turkey, emails: ayalcuk@gmail.com (A. Yalcuk), dogdu.gamze@gmail.com (G.D. Okcu)*
[b]*Department of Environmental Engineering, Izmir Institute of Technology, 35430 Urla, Izmir, Turkey, email: eserokten@gmail.com*

Received 12 April 2018; Accepted 24 October 2018

ABSTRACT

The photocatalytic degradation and mineralization of commercial solution of 2,4-dichlorophenoxyacetic acid (2,4-D) was carried out by UVA/P25 TiO_2 and UVA/P25 TiO_2/H_2O_2 oxidation processes under batch-mode conditions. In UVA + TiO_2 photocatalysis (TiO_2 1.5 gL^{-1}, pH 5, initial 2,4-D 25 mg L^{-1}), 97.47% ± 0.27% degradation, 39.89% ± 3.42% mineralization, and 65.52% ± 4.88% oxidation were achieved in 180 min, and in UVA +TiO_2 + H_2O_2 photocatalysis (TiO_2 1.5 g L^{-1}, pH 5, initial 2,4-D 25 mg L^{-1}, H_2O_2 150 mg L^{-1}), 99.74% ± 0.08% degradation, 55.99% ± 2.67% mineralization, and 82.49% ± 1.90% oxidation were obtained in 180 min. The pseudo-first-order kinetic model fitted the experimental data well, and the photocatalytic degradation process was explained by the modified L–H model; k_c and K_{LH} were 1.293 mg L^{-1} min^{-1} and 0.232 L mg^{-1}, respectively. Fourier transform infrared (FTIR) spectroscopy spectra and scanning electron microscopy (SEM) analysis indicated degradation of organic bonds of the herbicide and adsorption of 2,4-D particles onto the TiO_2 catalyst during 24-h experiments. Moreover, the dependence of k_{app} on the half-life time was determined by calculating the electrical energy per order (E_{EO}). UVA/TiO_2/H_2O_2 photocatalysis may be applied as a pretreatment to 2,4-D herbicide wastewater at a pH of 5 for biological treatment.

Keywords: 2,4-dichlorophenoxyacetic acid (2,4-D); Cost analysis; Electrical energy per order; Photocatalytic degradation; Mineralization; UVA/TiO_2/H_2O_2

1. Introduction

Generally, many kinds of pesticides are used to control a variety of pests that can damage crops and livestock and reduce productivity in the intensive modern agricultural activities needed for a growing population and to satisfy a high demand for food. However, in recent years, there has been an increasing concern among scientific communities and global agencies (such as EPA and WHO) on the use of pesticides due to their high risks to human health and the environment [1]. Active ingredients in pesticides are often toxic to living organisms and resistant to biodegradation, while the major sources of pesticides may leach into groundwater and reach surface water through direct surface runoff, disposal of empty containers, spraying, equipment washing processes, or effluents from pesticide formulating and manufacturing processes where they disturb the natural balance of ecosystems [2–4]. As a consequence of these agricultural activities, pesticide concentrations can reach levels beyond Turkish legislation limits (0.1 μg L^{-1}) in drinking water [5].

In many regions of the world and especially in Turkey, 2,4-dichlorophenoxyacetic acid (2,4-D) has been one of the most widely used chlorinated phenoxy alkanoic herbicides for controlling broad-leaf weeds in a variety of agricultural activities – including gardening – due to its high efficiency and low cost, especially in potato, grain, and corn production [6–8]. 2,4-D is considered moderately toxic (class II) by

* Corresponding author.

WHO, and its carcinogenic, neurotoxic, and endocrine disruptive potential cannot be neglected [6,9,10]. Recently, some studies stated the cardiotoxicity and genotoxicity of 2,4-D on zebra fish [11]. Since this compound is mostly degraded to its anionic form – which exhibits high water solubility (667 mg L^{-1}), high mobility, and extended lifetime – its continuous use may cause soil percolation, and surface and groundwater contamination. Moreover, 2,4-D is often detected in surface (≈6 μg L^{-1}) and drinking water (2.2–3.2 μg L^{-1}) sources [12,13]; the half-life of 2,4-D in the environment is relatively short, averaging 10 days due to its susceptibility to biological treatment in soils [14] and less than 10 days in water. The regulatory standard for 2,4-D in drinking water is 70 μg L^{-1} as per the US standard [15]. Moreover, the bio-refractory nature of chlorophenoxy herbicides requires development of novel treatment technologies to remove this type of herbicides from contaminated water and soil [15].

In recent years, by producing •OH^- radicals through chemical, photochemical, photocatalytic, and electrochemical reactions, advanced oxidation processes (AOPs) have become a promising technology to eliminate pesticides from water systems [2,16]. Among various semiconducting materials, P25 TiO_2 (anatase) has proven to be the most favorable semiconductor photocatalyst for wastewater treatment applications and offers several advantages: (i) high reactivity under UV light; (ii) chemically stable and harmless; (iii) superior photocatalytic oxidation ability and optical and electrical properties; (iv) lack of mass transfer limitations, long lifespan, and operation at ambient conditions; and finally (v) lower energy consumption compared to UV photolysis – as the necessary light intensities are lower [17,18]. Moreover, it is nontoxic, chemically inert, and inexpensive, and it does not undergo photocorrosion. The operating principle of heterogeneous photocatalytic oxidation has been thoroughly explained before [19–21]. The process relies on subsequently generating a superoxide radical anion ($O_2^{\bullet-}$) and hydroxyl radicals ($OH^{\bullet}$), which are the primary oxidizing species in photocatalytic oxidation processes [19]:

$$TiO_2 + h\nu \rightarrow e_{cb}^- + h_{vb}^+ \quad (1)$$

$$O_2(\text{oxygen molecule}) + e_{cb}^- \rightarrow O_2^{\bullet-}(\text{dioxide}(1-), \text{superoxide anion}) \quad (2)$$

$$O_2^{\bullet-}(\text{dioxide}(1-), \text{superoxide anion}) + H_2O \rightarrow OH^{\bullet}(\text{hydroxyl radical}) + OH^-(\text{hydroxyl ion}) + O_2(\text{oxygen molecule}) + HO_2^-(\text{hydrogen dioxide}(1-)) \quad (3)$$

$$H_2O + h_{vb}^+ \rightarrow OH^{\bullet}(\text{hydroxyl radical}) + H^+ \quad (4)$$

As reported in several previous studies, although the initial disappearance of the pollutant was rapid, a number of by-products were formed that might potentially be harmful to the environment [2,4,19,22]. In Turkey, formulation grade pesticides are directly and unconsciously applied to fields without complying with legal restrictions, and a major part of the pesticide industries are formulating units. There are many new studies on 2,4-D elimination in published literature, as it is the most widely used herbicide in the world, and the prohibition or limited usage of it by EPA and other organizations is still controversial [3,23–26]. However, only very limited studies have been previously published about photocatalytic treatment of ultra-pure 2,4-D herbicide, and these studies were only concerned with the determination of the influencing factors in the photocatalytic process and identification of the intermediate products [27–30]. So far, no extensive mineralization studies of photocatalytic degradation of formulation grade 2,4-D herbicide have been reported that have aroused interest or destroyed the parent compound. Also, commercial grade herbicide is preferred for agricultural activities instead of the pure form of 2,4-D, due to higher water solubility and lower cost.

This study focused on the degradation of commercial grade 2,4-D by UVA/TiO_2 and UVA/TiO_2/H_2O_2 in an aqueous matrix under varying conditions. The objectives of this study were: (i) to investigate the extent of mineralization and produce kinetic studies of 2,4-D by performing total organic carbon (TOC) and chemical oxygen demand (COD) analysis and mass spectroscopy, (ii) to propose adsorption of 2,4-D on P25 TiO_2 using scanning electron microscopy (SEM) and perform degradation of 2,4-D using a Fourier transform infrared (FTIR) spectroscopy method, (iii) to ensure the primary photocatalytic transformation of intermediates of the parent compound by liquid chromatography–electrospray ionization–tandem mass spectrometry (LC–ESI–MS/MS) techniques, and (iv) to look at the cost of applying photocatalytic systems with calculations based on the results, since economic aspects and energy consumption also have to be considered for such a process in terms of engineering applications.

2. Materials and methods

2.1. Chemicals

All chemicals employed in this investigation were used without further purification. Titanium (IV) oxide nanopowder (AEROXIDE® P25 ≥ 99.5%, 21 nm, 35–65 m^2 g^{-1} (BET)) was used as a photocatalyst (from Sigma Aldrich, Germany) due to its availability and high performance in photocatalytic degradation reactions. X-ray diffraction (XRD) analysis demonstrated that TiO_2 nanopowder was in anatase phase (Fig. S1). Commercial grade Amin EXT 500 SL (equivalent to 500 gL^{-1} 2,4-D) 2,4-D amine salt ($C_{10}H_{13}Cl_2NO_3$, Mw: 266.12 g mol^{-1}) was obtained from the Agrofarm® Company (Fig. 1). Other chemicals, including hydrogen peroxide solution of analytical purity 30% (w/w), NaOH, and H_2SO_4 (essay 97%) used for adjusting the pH, were obtained from

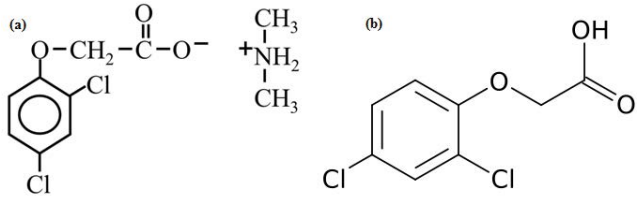

Fig. 1. Molecular structure of (a) 2,4-dimethylamine herbicide and (b) 2,4-D herbicide.

Merck (Germany). All solutions and reaction mixtures were prepared with purified water (Merck Millipore, spec. resistivity: 18.2 MΩ cm).

2.2. Experimental procedure

Photocatalytic experiments were performed in a 4.6 L (operating volume: 1 L) cylindrical batch photoreactor (14 cm D × 30 cm L) (Fig. 2) maintained at 22°C ± 1°C. The photoreactor is constructed from three parts: (i) an exterior Pyrex glass; (ii) a Pyrex glass thimble, where the upper part is fitted to the outside of the container to form a gastight seal, and running water is passed through the thimble to cool the reaction solution; and (iii) an empty quartz chamber, into which a Philips PL-L UVA 36 W lamp (315–38 nm; 110 μW cm^{-2}) was fitted. The reactor was also equipped with a control system, a water level sensor system, and a water inlet–outlet and gas inlet openings to supply air from a diffuser system with a capacity of 3.5 L min^{-1} during the experiments. The reactor was wrapped with aluminum foil to prevent UV ray penetration. For irradiation experiments, the desired 2,4-D concentration was prepared from a 100 mg L^{-1} stock solution daily in amber glass vessels, and the system was stirred and aerated in order to increase the oxygen transfer to the solution following the addition of TiO_2 for at least 30 min in the dark to allow the system to reach equilibrium in case of adsorption. This time was selected so that, under stirring in the dark, no more herbicide molecules could be adsorbed by the photocatalyst. Then, the UV light was turned on that signals the photocatalysis. At 0, 5, 10, 15, 30, 45, 60, 90, 120, 180, 300, 420, 540, 720, and 1,440 min, 50 mL 2,4-D solution samples were collected and filtered through 0.45 μm Millipore filters to remove TiO_2 particles for further analysis.

TiO_2 catalyst loading (0, 0.5, 1.0, 1.5, and 2.0 g L^{-1}), pH (3, 5, 7, and 9), and initial concentration of 2,4-D (10, 25, 50, and 100 mg L^{-1}) were analyzed to determine the optimum degradation of 2,4-D herbicide conditions. As preliminary studies for comparison, photolysis (irradiation without adding TiO_2) and adsorption (without irradiation) experiments were also performed. Photocatalytic experiments were repeated three times to check repeatability of the experimental results. The mineralization experiments were duplicated for 24 h.

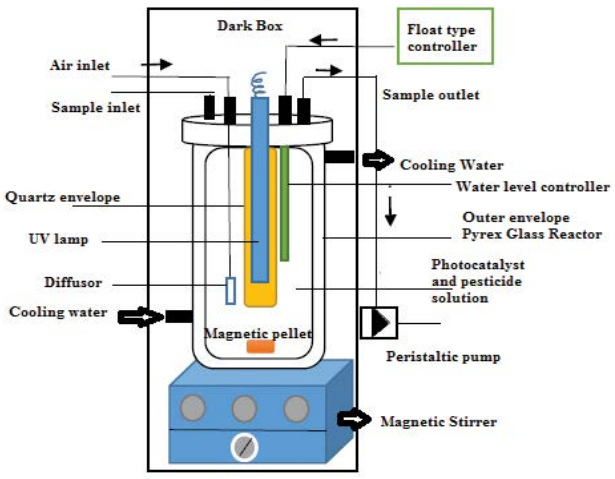

Fig. 2. Experimental setup of photocatalytic reactor.

2.3. Analytical methods

Optimization of the photocatalytic conditions was initially done using a spectrophotometer between 190 and 1,100 nm (Shimadzu UV-1601-PC) and measuring the optical density (OD) of the samples at 283 nm (Fig. S2), which is the given maximum absorption wavelength for the 2,4-D molecule. This was also confirmed by a spectrum reading from the spectrophotometer. A calibration curve was prepared between 0 and 50 mgL^{-1} for standard pesticide solutions in accordance with the relationship between absorbance and concentration that obeys the Lambert–Beer law. COD was measured using COD test kits (Test Kits No: 1.14541 from Merck, Germany) with a UV spectrophotometer (Pharo 100). A 3 mL sample was measured over 120 min at 150°C under thermoreactor (Merck Spectroquant TR 320) treatment. When the sample contained hydrogen peroxide (H_2O_2), interference in COD determination was reduced by increasing the pH to above 10 – to decompose hydrogen peroxide to oxygen and water [31]. The total organic carbon (TOC) was analyzed by NPOC method (680°C, 150 mL min^{-1}, an injection volume of 20 μL, a spray gas flow of 80 mL, and a spray time of 1.5 min) using a Shimadzu TOC-L analyzer with 20 mL sample. The adsorbable organic halogen (AOX) concentration analysis was carried out using a Behr CL 10 device with 3 mL sample. The pH and temperature measurements of all samples from the photocatalytic reactor were measured using a pH meter (Orion Star A329 Thermo Scientific) and a pH probe (8107UWMMD ROSS pH/temperature electrode). A LC–ESI–MS/MS instrument was used (Thermo TSQ Quantum Access Max LC-ESI-MS/MS) to verify the degradation of the 2,4-D into intermediate substances to identify the metabolites and to determine the residual herbicide concentration using the AOAC Official Method 2007.01 (the mobile phase of A: 5 mM ammonium formate and 0.1% formic acid (95:5 water:MeOH); and the mobile phase of B: 5 mM ammonium formate and 0.1% formic acid (5:95 water: MeOH)) with 10 mL sample. The adsorption of the 2,4-D herbicide molecule trapped on the TiO_2 catalyst was photographed with a scanning electron microscope (SEM, Jeol 6390-LV (20 kV, resolution: 3 nm)) during pre-photocatalytic and post-photocatalytic treatment. FTIR analysis was performed using a Shimadzu IR Prestige 21 high-resolution DLATGS detector to observe the changes in the functional structure of the 2,4-D herbicide before and after the photocatalytic treatment (at the end of the 24-h operation). Small amount of KBr powder was taken and fused into the disk to make it completely smoothened; 1 mL of the 2,4-D herbicide sample before and after the photocatalytic treatment was placed on the FTIR device and the spectrum was run.

3. Results and discussion

3.1. Preliminary studies

The available removal mechanisms for commercial 2,4-D herbicide mainly comprise stirring in the dark using spectrophotometric analyses and adsorption onto TiO_2,

photolysis with UV, and photocatalysis with TiO_2 and UV. In the experiment in which TiO_2 and UV were used together, a maximum of 85.77% ± 0.73% of the initial 25 mg L^{-1} of the 2,4-D concentration was removed in 15 min (data not shown). The degradation efficiency for photolysis was 13.64% ± 0.92% in 30 min, while the adsorption efficiency only reached 9.78% ± 1.47% in 30 min. Djebbar et al. [29] reported that only 4% of the 2,4-D was adsorbed after 50 min under dark conditions. Daneshvar et al. [32] determined that 93% of the herbicidal erioglaucine was removed in 20 min in the presence of P25 TiO_2 and light, whereas with direct photolysis without TiO_2, only 3% of the erioglaucine – a negligible amount – was removed. In this study, the adsorption experiments showed that approximately 14.81% of the 2,4-D herbicide was initially (at time zero) removed and 37.14% herbicide adsorption was achieved after 15 min. However, after 30 min, only 9.78% ± 1.47% herbicide removal was observed on the TiO_2 surface, which indicates that equilibrium conditions were achieved. The low 2,4-D adsorption level on the catalyst surface is attributable to the presence of hydroxyl radicals in the main degradation mechanism during the removal of the pollutant [33]. In other words, the experiments revealed the importance of using UV light and photocatalyst together for 2,4-D degradation.

3.2. Effects of TiO_2 on the degradation process

The concentration of TiO_2 as a photocatalyst has an important role in the efficiency of the photocatalytic process. The effect of different doses of catalyst from 0 to 2.0 g L^{-1} was tested with an initial 100 mg L^{-1} concentration of 2,4-D at a pH of 3 (Fig. 3). Batch experimental analysis was begun at a pH of 3, which is close to the pKa value of 2,4-D herbicide (pKa = 2.73) [34]. As shown in Fig. 3, with increasing catalyst concentration at 1.5 gL^{-1}, the reaction rate increases, because with an increasing amount of catalyst more 2,4-D molecules are adsorbed onto the catalyst surface and herbicide removal in the area of irradiation increases. However, it was observed that above a certain concentration (1.5 g L^{-1}), the herbicide concentration levels off and becomes independent of the catalyst concentration. This limit is reported to depend on the geometry and working conditions of the photoreactor and for a defined amount of TiO_2 [19]. The TiO_2 particles become saturated with the degrading molecules, and increasing the catalyst concentration beyond a certain limit – which is 1.5 g L^{-1} in this case – does not increase the photodegradation efficiency. Also, further increasing the TiO_2 concentration may result in the formation of catalyst clusters leading to active sites on the catalyst surface that are inaccessible [35,36]. Therefore, 1.5 g L^{-1} of TiO_2 was selected as the optimum amount of photocatalyst. Fig. 3 also shows maximum removal at 15 min for all the studied catalyst concentrations before an increase in optical density is observed. As photocatalysis proceeds, many intermediate molecules are formed and these intermediates may also be measurable at 283 nm, causing interference. Also, Oh and Tuovinen [37] stated in their articles that although UV spectrometry is a relatively fast and sufficient method, it is not suitable to quantify 2,4-D if UV-absorbing intermediates accumulate. Like other studies in the literature, the temperature variation in the reactor was 22°C ± 1°C, and it had no significant effect on photocatalytic reactions, which rely upon radicals for degradation, and those radicals cannot be formed by such a small input of thermal energy [38].

3.3. Effects of pH on the degradation process

The pH of the medium affects the performance of the adsorption/desorption processes and the apparent separation of the "photogenized" electron–hole pairs [39]. The load on the TiO_2 surface depends on the pH as a result of the amphoteric properties of the surface [40]. The surface load and flat-band potential of the photocatalysts largely depend on the pH value. The electrostatic attraction and repulsion between the catalyst surface and organic molecules depend on the ionic form of the organic compound (anionic and cationic), and they develop under the influence of pH. The pH affects TiO_2 aggregation, while the interaction between solvent molecules, catalyst and radicals – or the intermediate products – occurs during the photocatalytic process [4]. Since changes in solution pH have a significant impact on the photocatalytic process that reflects the surface charge properties of the photocatalyst, a pH range from 3 to 9 was investigated. The highest removal was observed at a pH of 5 (Fig. 4). The zero point of charge (pH_{zpc}) for P25 TiO_2 is at a pH of 6.25, and hence, the highest removal was seen at a pH

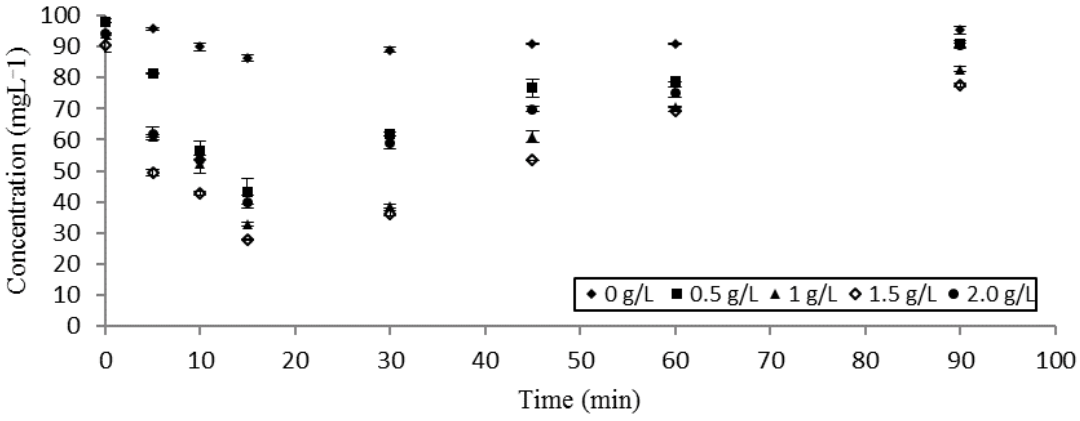

Fig. 3. Effects of the amount of TiO_2 on concentration removal of 2,4-D herbicide, C_0:100 mg L^{-1}, pH 3, 150 rpm, 22°C ± 1°C.

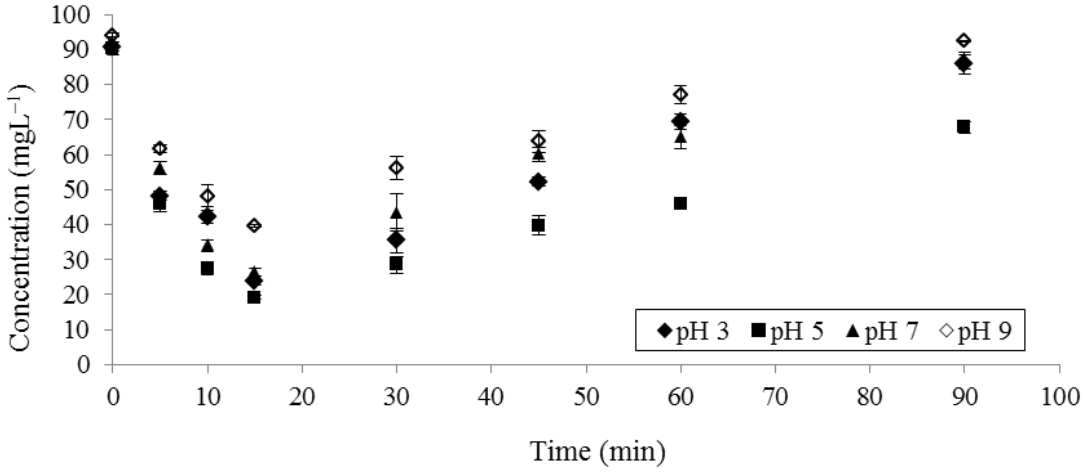

Fig. 4. Effect of pH during photocatalysis, C_0:100 mg L^{-1}, 1.5 g L^{-1} TiO_2, 150 rpm, 22°C ± 1°C.

value lower than the pH of the zero point of charge. The TiO_2 surface will be positively charged at pH values below 6.25, while it is negatively charged at pH values above 6.25. The pKa value of 2,4-D is 2.73 [34]; at a lower pH value, positively charged, protonated 2,4-D becomes predominant and at a higher pH value, negatively charged 2,4-D is predominant. Therefore, at a pH of 5, the electrostatic interaction leads to greater adsorption of the negatively charged herbicide onto the positive TiO_2 surface and therefore increases degradation efficiency. As expected, maximum removal conditions will be at $pK_a^{2,4\text{-D}} < pH < pH_{ZPC}^{TiO2}$ [41].

3.4. Effects of initial herbicide concentration on the degradation process

In order to investigate the effectiveness of photocatalytic oxidation with increasing herbicide concentration, experiments were conducted for 10, 25, 50, and 100 mg L^{-1} concentrations of 2,4-D with a P25 TiO_2 catalyst (1.5 g L^{-1}) at a pH of 5. Herbicide removal efficiencies were comparable and in a range from 81% to 86% for the studied concentrations, except for 10 mg L^{-1}, which turned out to be a too low a concentration to work spectrophotometrically (Fig. 5). It should be noted that measured concentrations at time zero were always lower than the initial concentrations; the difference was believed to be the adsorption onto the TiO_2 particles during the 30 min of stirring in the dark. The best photodegradation efficiency was with 25 mg L^{-1} (85.77% ± 0.73%), and as the concentration increased fourfold to 100 mg L^{-1}, the removal efficiency decreased to 80.78% ± 0.63%. Although the magnitude of decrease may seem insignificant, it may be explained by the limited availability of the photocatalytic surface due to the adsorption of herbicide for increased herbicide concentrations [19].

Blockage of the photocatalyst's active sites by herbicide molecules, and subsequently higher absorption of UV light by the herbicide rather than by TiO_2, was also reported previously [41,42]. Also, given that the same concentration of catalyst was used for the experiments, less available sites with increased herbicide concentration would result in fewer numbers of 2,4-D molecules affected by OH^-. Higher herbicide concentrations may also interfere with the absorption of UV light, and thus, photons may not be able to reach the catalyst surface, resulting in decreased removal efficiency [41,43,44].

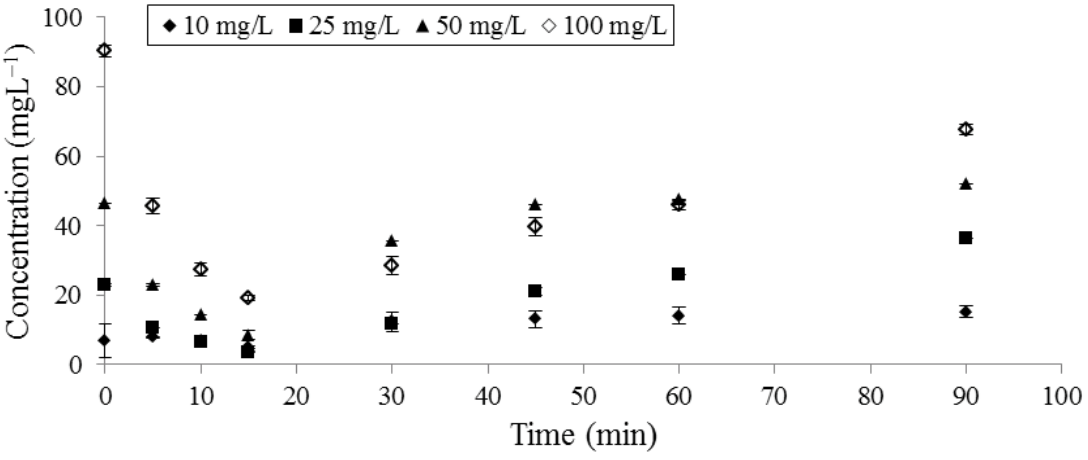

Fig. 5. Effects of substrate concentration on photocatalysis, pH 5, 1.5 g L^{-1} TiO_2, 150 rpm, 22°C ± 1°C.

3.5. Effects of initial H_2O_2 concentrations on the degradation process

Since hydroxyl radicals are known to play an important role in photocatalytic degradation, the addition of electron acceptors such as hydrogen peroxide will enhance the formation of hydroxyl radicals [19]. In our case, as shown in Fig. 6, the photocatalytic degradation of 25 mg L^{-1} of 2,4-D in the presence of 1.5 g L^{-1} of TiO_2 P25 at a pH of 5 has been studied at different H_2O_2 concentrations (50–200 mg L^{-1}).

There are two important roles for H_2O_2 in the photocatalytic degradation: (1) it accepts a photo-generated electron from the conduction band and thus promotes the charge separation (Eq. 5), and (2) $OH^{\bullet}$ (hydroxyl) radicals are formed via interaction with the O_2^- (dioxide (1-)) species in the superoxide mechanism (Eq. 6) [4] :

$$H_2O_2 + e^- \rightarrow HO^-(\text{hydroxyl ion}) + HO^{\bullet}(\text{hydroxyl radical}) \quad (5)$$

$$H_2O_2 + O_2^-(\text{dioxide}(1-)) \rightarrow HO^{\bullet}(\text{hydroxyl radical}) + HO^-(\text{hydroxyl ion}) + O_2(\text{oxygen}) \quad (6)$$

Fig. 6 shows the decrease in the removal efficiency of 2,4-D with an increase in the H_2O_2 concentration to 200 mg L^{-1}. As the H_2O_2 concentration increases, the H_2O_2 in the medium starts to separate and inhibits hydroxyl radical formation and photocatalytic degradation, or OH reacts with excess H_2O_2 and forms HO_2 [45]. Alalm et al. [46] reported the maximum degradation efficiencies for lambda-cyhalothrin, chlorpyrifos, diazinon, and COD as 68.9%, 73.3%, 49.1%, and 84%, respectively. Furthermore, by using the UV/TiO_2/H_2O_2 system instead of UV/TiO_2 system, the removal efficiencies for lambda-cyhalothrin, chlorpyrifos, diazinon, and COD were increased by 8%, 13%, 11%, and 5%, respectively. Aye et al. [47] stated that an increase in H_2O_2 concentration, from 15 to 25 mM, resulted in a reduction in degradation due to the formation of undesirable by-products, which in turn encumbered effective UV adsorption by the oxidant. Since H_2O_2 may be preferred over oxygen as an electron acceptor, electron–hole recombination may be inhibited at low H_2O_2 concentrations [48]. Various experiments were carried out at the optimum H_2O_2 concentration of 150 mg L^{-1}. Moreover, in the presence of 2,4-D and H_2O_2 in the solution, and the absence of TiO_2 and lighting, no visible compound loss was observed.

3.6. Pesticide mineralization in aqueous solution under optimum operating conditions

In AOP-based systems, the complete mineralization of target pollutants is a critical issue that requires attention. Incomplete mineralization indicates the presence of residual by-products in the system, which may be more toxic or less toxic than the parent compound [49,50].

In the first step, photocatalytic oxidation experiments were carried out until 2,4-D was totally eliminated, and its mineralization was complete in order to get information on kinetics (Fig. 7). The relationship between the photodegradation efficiency of 2,4-D and the illumination time was investigated by fixing the pH at 5, with a 25 mgL^{-1} herbicide concentration and a 1.5 g L^{-1} TiO_2 concentration. The LC–ESI–MS/MS analyses showed that the degradation efficiency of 2,4-D at 180 min was 97.47% ± 0.27% (Fig. 7). Djebbar et al. [29] reported that, at a pH of 4.2, 5×10^{-4} M of 2,4-D was rapidly degraded in approximately 100 min. The oxidative power of the $OH^{\bullet}$ radicals formed during photocatalysis is known to be strong enough to oxidize 2,4-D with CO_2, H_2O, and other mineral acids [51]. As seen in Fig. 7, during the period between the 60th minute and the 180th minute, photodegradation of only 5% of 2,4-D was achieved. This is possibly due to the production of small organic molecules in large amounts and their adsorption onto the TiO_2 surface with increasing illumination time, which leads to the formation of $HO^{\cdot}$ radicals that bond with 2,4-D molecules.

Mineralization was investigated by measuring COD and TOC. The decrease in COD is also a sign of the mineralization or degradation degree of an organic species [52]. The decrease in TOC during the illumination period indicates the conversion of 2,4-D to by-products with photo-oxidation, and its conversion to CO_2 and H_2O, as the reaction continues [53]. With the 24-h photocatalysis experiment, removal of 53.04% ± 3.14% TOC was achieved. After 180 min, the lowest COD concentration was 20 ± 2.83 mg L^{-1}, which corresponds to a TOC concentration of 13.56 ± 0.77 mg L^{-1} (Fig. 8). Getting as high as 65.52% ± 3.88%, a significant amount of the organic

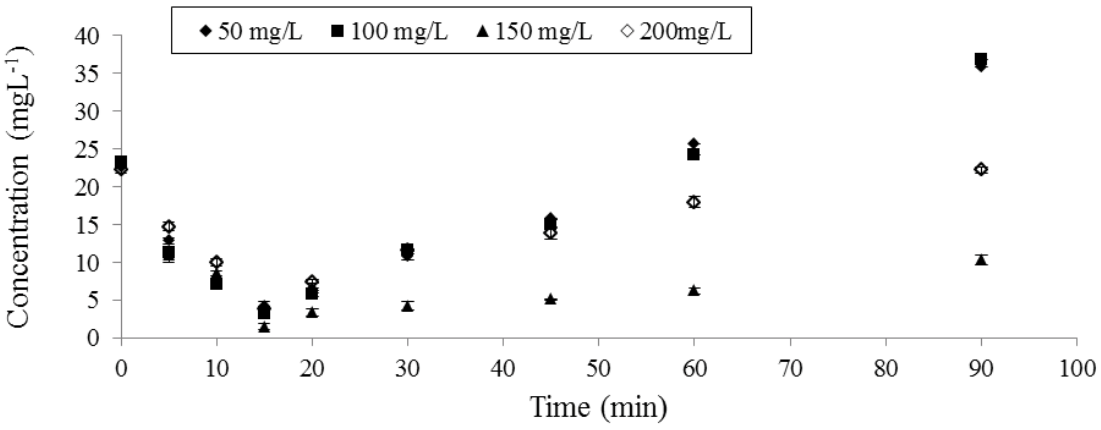

Fig. 6. Effects of H_2O_2 concentration on photocatalysis, *C*: 25 mg L^{-1}, pH 5, 1.5 g L^{-1} TiO_2, pH 5, 150 rpm, 22°C ± 1°C.

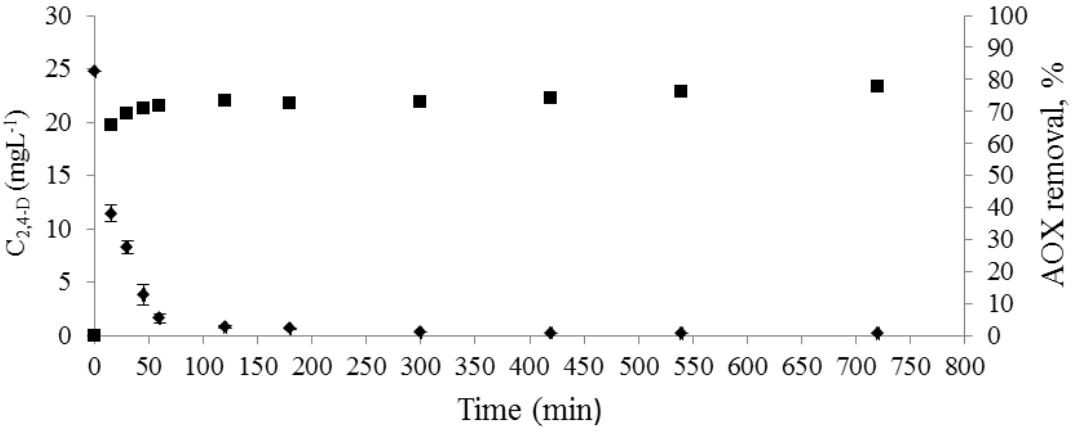

Fig. 7. 2,4-D concentration profile during the photodegradation of 2,4-D (•), AOX removal, % profile (■) (C_0 = 25 mg L^{-1}).

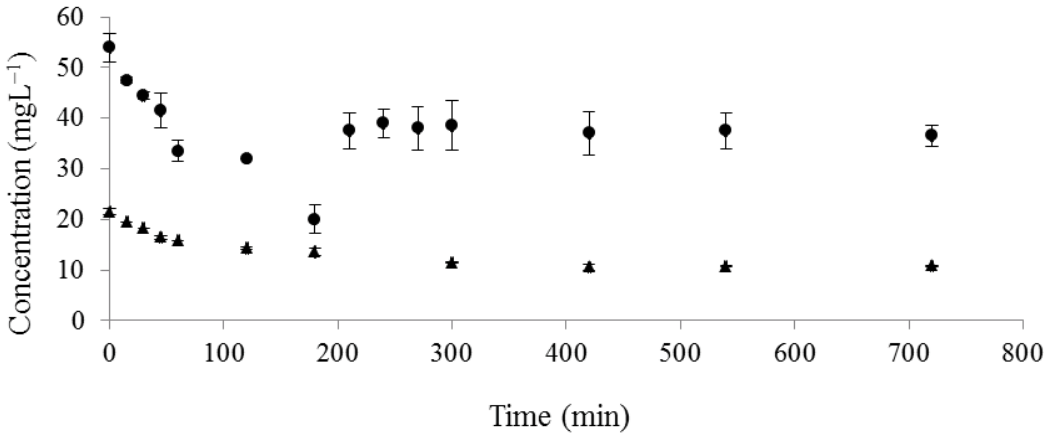

Fig. 8. COD (•) and TOC (▲) profiles during the photocatalytic degradation of 2,4-D (C_0 = 25 mg L^{-1}).

matter content of the initial COD concentration was removed after 180 min, which was also confirmed by the TOC removal.

Oxidation of the target compound was expected to modify its chemical structure and result in a COD decrease. More importantly, biodegradability of photocatalytic products becomes important for the biological stage that will follow this study. So, an increase in oxidation of the target compound (COD decrease) with limited mineralization (low TOC decrease) is a favorable trend to understand significant residual organic compound in microbial cultures [54]. Finally, a favorable trend is a decrease in the ratio of COD/TOC during the photocatalytic degradation of a target compound—in other words, 2,4-D herbicide (Fig. 8). COD removal was maximum where the majority of 2,4-D was eliminated and then the COD value increased and was stable afterwards – probably due to the formation of stable by-products. Finally, two time points were determined, one determined spectrophotometrically (at 15 min) and the other determined through measuring COD/TOC (at 180 min), to see if they might be producing two different and possibly favorable influents for second-step treatments, such as biological treatments.

Despite the conversion of 53.04% ± 3.14% of the initial carbon content of 2,4-D to CO_2 after 24 h, the photocatalytic mineralization of 2,4-D was completed (Fig. 8). This is attributable to the formation of organic by-products during the period from the degradation of the first molecule to total mineralization. Longer illumination periods are required to achieve complete mineralization under the stated experimental conditions [55]. The most important photocatalytic oxidation pathway for phenoxy herbicides is the degradation of the carbon–oxygen bond in the aromatic chain [53]. This step is considerably speedy and, as seen in Fig. 8, results in the rapid degradation of 2,4-D. The rapid degradation of the 2,4-D herbicide can be attributed to the chlorine atoms in its structure, which lead to the easy oxidation of 2,4-D through photocatalysis during the low light period [56]. Obtaining the greatest degradation of the 2,4-D concentration after 180 min is associated with the formation of 2,4-dichlorophenol, which is the largest and more toxic and more stable by-product of 2,4-D, as determined by the results obtained with LC–ESI–MS/MS [53]. In this study, the LC–ESI–MS/MS analysis revealed that the products formed after the degradation of 2,4-D (m/z = 221.0) with UV/TiO_2 and UV/TiO_2/H_2O_2 mostly comprised 2,4-dichlorophenol (2,4-DCP) (m/z 163.0) and contained small quantities of 2,4-dichloro-1-methoxy benzene (2,4-DCA) (m/z = 176.0) and 4-chlorophenol (4-CP) (m/z = 128.50). In their study, Singh and Muneer [28] obtained various by-products by performing the GC–MS analysis of 2,4-D in the presence of P25

catalyst; the by-products included 2,4-dichlorophenol (2,4-DCP), 2,4-dichloro-1-methoxybenzene benzaldehyde, benzyl alcohol, 3,5-dichlorobenzene-1,2-diol, 4-chlorophenol (4-CP), 4-6-dichlorobenzene-1,3-diol, and 3-chlorobenzene-1,2-diol. The researchers attributed the formation of 2,4-dichlorophenol to the bonding of OH radicals to the alkyl chain in the molecule and stated that 2,4-dichlorophenol was the first of the main by-products of 2,4-D [27,28].

The photodegradation efficiency of the 2,4-D herbicide was analyzed using an optimum H_2O_2 concentration of 150 mg L^{-1}, 25 mg L^{-1} herbicide, a TiO_2 concentration of 1.5 g L^{-1}, and a pH of 5; the removal of 92.05% ± 0.03% was achieved after 15 min. After 180 min, 2,4-D was completely degraded (Fig. 9). Therefore, the rate of 2,4-D photodegradation was considerably higher when UVA lighting, optimum concentrations of peroxide and TiO_2, and an optimum pH were used. The halogen bond in the organic molecule gives rise to the main toxicity of the halogenated organic compounds, and, economically speaking, the complete degradation of the organic compound is therefore not necessary [57]. As seen in Fig. 7, the removal of adsorbable organic halogen in the first mineralization experiment without peroxide was 77.67%, while, in the experiments with H_2O_2, it reached a maximum of 79.14% after 24 h (Fig. 8). The AOX profiles in both figures reveal that 2,4-D degradation was completed within the first 60 min, while the AOX removal was almost completed and reached a constant value after 1 h. In their study, Catalkaya and Kargi [58] stated that the first reaction involved the degradation of diuron to by-products and its dehalogenation (AOX removal) occurred considerably faster. The second reaction is mineralization (TOC removal) and it occurs slowly. In the same study, the researchers reported that the time needed for the mineralization of diuron exceeded 60 min, but dehalogenation of diuron occurred in 5 min; the researchers attributed this to the by-product formation during the oxidation process.

According to Fig. 10, in the 24-h photocatalysis experiment, in which 150 mg L^{-1} of H_2O_2 was used, a maximum COD removal of 85.19% ± 0.95% was achieved after 150 min, and COD removal remained stable until the 24th h. Moreover, with the photocatalytic process, 55.99% ± 1.32% TOC removal occurred after 180 min. Compared to the mineralization experiment without peroxide – as given in Fig. 7 – through maximum mineralization in a shorter period, the use of peroxide resulted in the degradation of the stable by-products that occur after 180 min. Nyugen et al. [59]

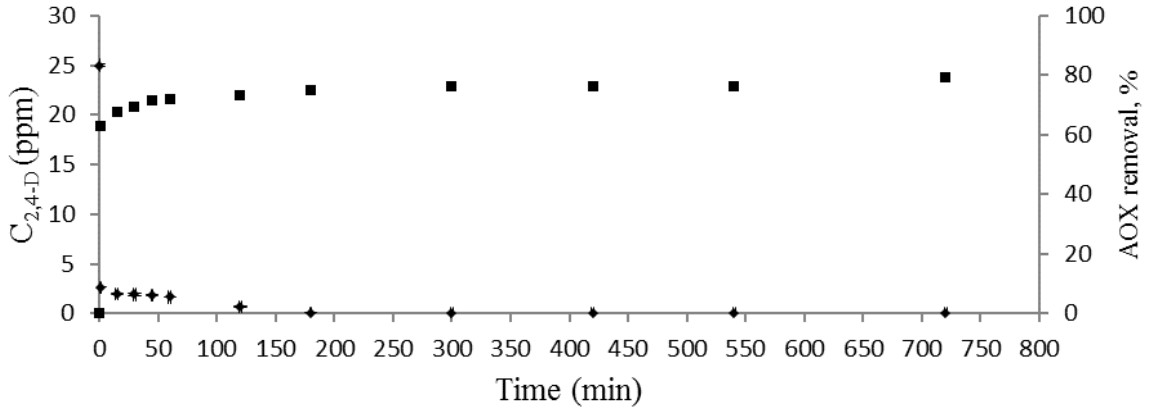

Fig. 9. 2,4-D concentration profile during the photodegradation of 2,4-D (◆), AOX removal, profile% (■) (C_0 = 25 mg L^{-1}, 150 mg L^{-1} H_2O_2 concentration).

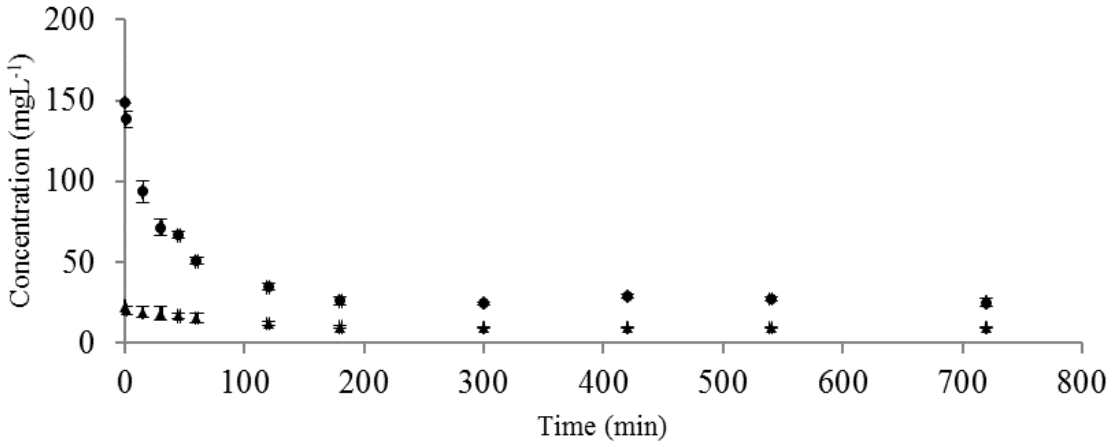

Fig. 10. COD (•) and TOC (▲) profiles during the photocatalytic degradation of 2,4-D (C_0 = 25 mg L^{-1}, 150 mg L^{-1} H_2O_2 concentration).

reported 14%, 11%, and 33% removal of phenol, o-cresol, and 4-chlorophenol (4-CP), respectively, within 3 h by direct photolysis with a 100 W UV lamp. The addition of 2.0 mM of H_2O_2 resulted in phenol, o-cresol, and 4-chlorophenol (4-CP) removal of approximately 55%, 52%, and 59%, respectively. Furthermore, by treating the solution with 1 g L^{-1} of TiO_2 under 100 W UV radiation, removal of phenol, o-cresol, and 4-chlorophenol (4-CP) reached 70%, 65%, and 74%, respectively. By combining the UV/TiO_2/H_2O_2 processes, 97% of phenol and 94% of o-cresol were degraded within 3 h, while 99% of 4-CP was degraded in a shorter radiation period of 2.5 h. The particle diameter of P25 is large and may result in hole production (h^+) at higher amounts in shorter periods. The holes react with the hydroxyl ions (OH^-) in the solution and produce hydroxyl radicals ($OH^\bullet$) that can oxidize the organic pollutants. In addition, the high reaction rate of P25 is most probably due to the quantum efficiency of P25. Therefore, at a higher efficiency, the hole will react with H_2O_2 and the polluting material itself [47]. In this study, with the UV/TiO_2 process, a maximum 2,4-D degradation efficiency of 99.82% ± 0.03% and a maximum COD value of 65.52% ± 3.88% were obtained, whereas during the 24-h mineralization period using the UV/TiO_2/H_2O_2 processes, a maximum 2,4-D degradation efficiency of 100% and a maximum COD removal of 85.19% ± 0.95% were reached. Although the degradation efficiency of the 2,4-D herbicide almost remained constant, the COD removal efficiency was increased by 19.67%. On the other hand, in the oxidation experiment without peroxide in Fig. 8, 30% of COD was removed after 180 min, while, in the oxidation experiment with peroxide in Fig. 10, the decrease in COD occurred more slowly in addition to the degradation of 2,4-D. At the end of the 3-h oxidation process, COD removal was completed in both cases. This was associated with an insufficient amount of $OH^\bullet$ radicals causing the degradation of the organic compounds, although the by-products were formed after 180 min. Incomplete COD removal is attributed to the toxicity of the by-products remaining after the photocatalytic treatment of 2,4-D [36]. Berberidou et al. [4] mentioned that the photocatalytic process was accelerated twofold in the presence of 0.5 gL^{-1} of TiO_2 P25 and 100 mgL^{-1} of H_2O_2. In general, strengthening the photocatalytic process with the addition of H_2O_2 contributes to the formation of new hydroxyl radicals in the presence of UVA radiation. Furthermore, in the photocatalytic process, H_2O_2 is a better electron acceptor than O_2 [59].

3.7. FTIR spectra and SEM analysis

FTIR analysis produces a spectral range from 750 to 4,000 cm^{-1}, which provides information on the changes in the functional structure of the 2,4-D herbicide occurring after a 24-h photocatalytic process. In Fig. S3, there are important peaks in the 2,4-D herbicide in the 400–4,000 cm^{-1} range. Fig. S4 shows the changes in the FTIR spectrum of the 2,4-D herbicide before and after the process.

The differences between the FTIR spectra of the treated and untreated solutions indicate the degradation of the organic bonds of the pesticides [18]. In Fig. S4, the peaks in the FTIR spectrum after the photocatalytic process show various similarities to the peaks of the original 2,4-D. In contrast to the peak of the original 2,4-D herbicide in Fig. S3 at 1,733 cm^{-1}, in Fig. S4, peaks were observed at 1,735.93 cm^{-1} at the 0^{th} min, at 1,747.93 cm^{-1} after 3 h, and at 1,737.86 cm^{-1} after 24 h. In their study, Trivedi et al. [25] reported that the peak they observed at 1,732 cm^{-1} indicated the presence of the carboxyl group C=O. In Fig. S3, bands at 1,311 and 1,095 cm^{-1} in the original 2,4-D spectrum signify the symmetrical and asymmetrical peaks of C–O–C. Moreover, the O–H deformation coupled with C–O stretching vibration is observed at 1,234 cm^{-1} [60]. The peaks at 1,470 and 1,428 cm^{-1} correspond to the C=C aromatic ring vibration and CH_2 alkane vibration, respectively [61]. The peak at 697 cm^{-1} corresponds to C–Cl stretching [25].

Scanning electron microscopy (SEM) shows the high homogeneity of the commercial P25 TiO_2 sample at the anatase phase with a mean particle size of 21 nm and 35–65 m^2g^{-1} BET surface area (Brunauer–Emmett–Teller surface area). The particles are spherical, and the nanoparticles with sizes smaller than 50 nm agglomerate [62,63]. SEM analysis is used to investigate the morphology, crystallinity, and surface area of materials. By analyzing the SEM images of the commercial P25 TiO_2 catalyst before and after the photocatalytic process, this study investigated the suitability of TiO_2 for the surface adsorption of the 2,4-D herbicide. Fig. 11(a) and (b) shows the SEM images of TiO_2 before and after the photocatalysis of the 2,4-D herbicide, respectively.

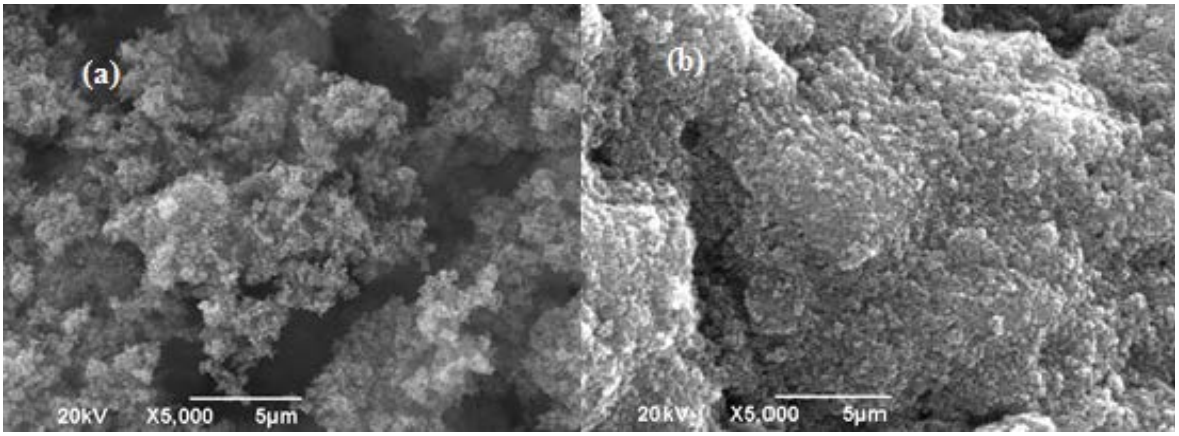

Fig. 11. SEM images of the P25 TiO_2 catalyst (a) before and (b) after the photocatalysis of 2,4-D herbicide.

As seen in Fig. 10(a), P25 TiO_2 catalyst was in the form of irregular and agglomerated crystal structure, while in Fig. 11(b), the density of the surface of the catalyst was increased following its coverage by particles of the 2,4-D herbicide after the photocatalytic process, and the surface became more compact and smooth. This led to the conclusion that the interparticle voids were probably filled with herbicide particles.

3.8. Kinetics of photocatalytic degradation

The Langmuir–Hinshelwood (L–H) equation is used to model the heterogeneous photodegradation kinetics of many organic pollutants under UV lighting and TiO_2 distribution, and it is the best model for explaining this process [55,59,64,65]. According to the L–H model, the photocatalytic reaction rate (r) is proportional to the fraction of the surface covered by the organic matter (θ_x), the reaction rate constant (k_r), the concentration of the organic species, and the Langmuir adsorption constant (K):

$$r = -\frac{dC}{dt} = k_r \theta_x = \frac{k_r K C}{1 + KC} \tag{7}$$

Challenges may arise when determining the kinetics of the process as a result of the formation of some by-products and the simultaneous adsorption and degradation during the photocatalytic process. Considering the smaller time interval, the change in the effect of the by-products can be neglected [2]; therefore, the photocatalytic degradation rate is expressed as a function of the 2,4-D concentration:

$$r = k_r \times \frac{K_c C}{1 + K_c C} \tag{8}$$

If the initial concentration is low, the k in the denominator is neglected. Hence, the rate apparently becomes a first-order equation that can be written as follows:

$$r = -\frac{dC}{dt} = k_r \theta = k_r k_c t = k_{app} t \tag{9}$$

Integrating Eq. (9) above using the boundary condition, that is, at $t = 0$, $C = C_0$; and $t = t$, $C = C$, it can be rewritten as Eq. (10):

$$\ln \frac{C}{C_0} = -k_{app} t \tag{10}$$

The apparent pseudo-first-order rate constant (k_{app}) was calculated from the slope of the plot, and values are given in Table 1. According to the k_{app} and regression coefficient (R^2) given in Table 1, pseudo-first-order kinetics can be employed to explain the adsorption and photo-oxidation mechanisms in the reactor. According to Table 1, when the 2,4-D concentration increased from 25 to 50 mg L^{-1}, the k_{app} value decreased because of the decreasing mass transfer flux in the photocatalytic process [2]. These slopes describe a linear behavior, and their linear regression coefficients are between 0.98 and 0.97 (Fig. S5.). These values are clear indicators of the compliance of the photodegradation reaction of the 2,4-D herbicide to the first-order kinetics. The pseudo-first-order kinetic modeling approach was reported to be suitable for the advanced oxidation processes [66] and with photocatalytic processes [67,68]. Moreover, the initial herbicide concentration has an important effect on the degradation rate. For example, kinetic rate constant decreases with increasing initial herbicide concentration [21,69]. According to Table 1, a low 2,4-D herbicide concentration shows a good consistency with a first-order reaction. Degradation rate largely depends on the formation of the hydroxyl radicals [44]. On the other hand, Vishnuganth et al. [2] stated that reaction rate constant will increase with increasing carbofuran removal efficiency. This is confirmed by the k_{app} values of 0.0441 and 0.0238 min^{-1} at two different 2,4-D pollutant concentrations of 25 and 50 mg L^{-1}, respectively. While the removal efficiency of 2,4-D after 60 min with the photocatalysis process reached 92.47% at 25 mg L^{-1} and decreased to 73.72% at 50 mg L^{-1}, the initial degradation rate (r_0) increased from 0.103 to 0.190 mg L^{-1} min^{-1} with increasing initial concentration. This implies the inadequacy of the first-order kinetic model under real conditions. At a low pollutant concentration, a great number of water molecules produce hydroxyl radicals through adsorption onto TiO_2, and thus, a rapid oxidation process occurs. As the concentration of the target pollutant increases, degradation rate decreases as a result of the increasing competition for adsorption between the pollutant and water molecules, and the resultant decrease in the formation of the hydroxyl radicals leads to the decrease in the number of the water molecules adsorbed onto the free TiO_2 active regions. In addition, since it causes competition in the active regions on the catalyst surface, the amount of by-product formation gains further importance for increasing pollutant concentrations [39].

In agreement with the results of this study, the study carried out by Bouafia-Chergui et al. [36] on the removal efficiency of tetracycline (TC) decreased from 99% to 85% at 5 and 20 mg L^{-1}, respectively, and the initial degradation rate of TC (r_0) increased with the increase in the initial concentration from 0.22 to 0.42 mg L^{-1} min^{-1}. Kamble et al. [70] reported that the photocatalytic rate constant decreased with the decreasing initial phenoxyacetic acid concentration. This behavior can be explained by the substrate molecules exceeding the sorbent capacity, which affects the degradation rate:

Table 1
The kinetic parameters obtained in the study

C_0 (mgL^{-1})	r_0 (mgL^{-1} min^{-1})	k_{app} (min^{-1})	$t_{1/2}$ (min)	$t^*_{1/2}$ (min)	R^2	k_c (mg L^{-1} min^{-1})	K_{LH} (L mg^{-1})
25	1.103	0.0441	15.71	11.98	0.98		
50	1.190	0.0238	29.12	21.65	0.97		
					1.00	1.293	0.232

$$\frac{1}{k_{app}} = \frac{1}{k_c K_{LH}} + \frac{C_0}{k_c} \quad (11)$$

Here, C_0 is the initial herbicide concentration (mg L^{-1}), K_{LH} is the L–H adsorption equilibrium constant (L mg^{-1}), and k_c is the surface reaction rate constant (in mg L^{-1} min^{-1}). According to Eq. (11), the plot of $1/k_{app}$ versus C_0 results in a linear change and confirms the relationship between the initial degradation rate and L–H adsorption. The terms k_c and K_{LH} are calculated using the slope and intersection of the line and were determined to be 1.293 mg L^{-1} min^{-1} and 0.232 mg L^{-1}, respectively. In the removal of carbofuran, Vishnuganth et al. [2] obtained k_c and K_{LH} values of 1.51 mg L^{-1} min^{-1} and 0.1942 mg L^{-1}, respectively. Bamba et al. [64] obtained a pseudo-first-order L–H-type rate coefficient value of k = 1.787 mg L^{-1} min^{-1} for P25 depending on the TiO_2-sensitized primary oxidation occurring on a monolayer surface, while obtaining a monolayer adsorption constant of K = 0.801 mg L^{-1} – relating to the pseudo-equilibrium constant. Daneshvar et al. [48] reported that the degradation rate of phosalone (a type of organophosphate pesticide) was high at the initial stages of illumination and gradually decreased over time. The rate constant of phosalone was determined to be 0.0532 min^{-1}. Moreover, Daneshvar et al. [32] reported the second-order degradation constant (k) and adsorption equilibrium constant (K) to be 0.984 mg L^{-1} min^{-1} and 0.116 mg L^{-1}, respectively, for erioglaucine.

Half-life ($t_{1/2}$) is defined as the time required for the initial 2,4-D concentration in the aqueous solution to be reduced by a half during the reduction process. By using Eq. (11) and replacing C_0 with $C_0/2$, $t^*_{1/2}$ is obtained:

$$t^*_{1/2} = \frac{C_0}{2k_c} + \frac{\ln 2}{k_c K_{LH}} \quad (12)$$

Alternatively, half-life time ($t_{1/2}$) is calculated according to the experimental data by using the pseudo-first-order rate constant (k_{app}):

$$t_{1/2} = \frac{\ln 2}{k_{app}} \quad (13)$$

According to Table 1, at the low initial 2,4-D concentration (25 mg L^{-1}), $t^*_{1/2}$ and $t_{1/2}$ were almost the same. As seen in Table 1, the difference between the estimated and observed half-life increases with increasing 2,4-D concentration [36]. This stems from the competition between the main pollutant and its products formed during the degradation with HO, while the consumption of radicals has a limiting effect [71]. As seen in Table 1, the half-life of the first-order reaction increases with increasing initial 2,4-D concentration, depending on the decrease in the k_{app} value.

3.9. Energy consumption and economic analysis

3.9.1. Electrical energy determination

The degradation of the 2,4-D herbicide by the photochemical process consumes electrical energy [2,72]. The electrical energy consumed by this process constitutes an important part of the operating cost. For a batch reaction, E_{EO} (kW energy amount consumed per process) is calculated using the following equation [32]:

$$E_{EO} = \frac{P \times t \times 1{,}000}{V \times 60 \times \log\left(\frac{C_0}{C_f}\right)} \quad (14)$$

The above equation is indirectly associated with the L–H model first-order kinetic:

$$\ln\left(\frac{C}{C_0}\right) = -k_{app} t \quad (15)$$

By coupling Eq. (14) with the L–H model first-order kinetic Eq. (15), E_{EO} can be represented as follows:

$$E_{EO} = \frac{38.4 \times P}{V \times k_{app}} \quad (16)$$

Equation (16) (E_{EO}) is used to determine the electrical energy model of each ideal batch reactor. Table S1 shows the E_{EO} values determined for the 2,4-D removal with the UVA/TiO_2 and UVA/TiO_2/H_2O_2 processes.

3.9.2. Total operating cost

Cost analysis is among the most important criteria in selecting the best wastewater treatment method. Advanced oxidation processes largely depend on electrical energy, which tends to be one of the major contributors to the operating cost [73,74]. The total cost is made up of investment cost, operating cost, and maintenance cost. Reactor configurations, and the concentration and structure of the pollutant are the main factors affecting the cost of classical wastewater treatment systems. The International Union of Pure and Applied Chemistry (IUPAC) proposed the figures-of-merit for the electrical energy consumption by advanced oxidation processes (AOP) [73]. Therefore, cost evaluation was performed based on "figure-of-merit (E_{EO})" for all the individual batch experiments [2,75,76].

Electrical energy consumption per process (E_{EO}) compares the electrical efficiency of various UV-based AOPs with each other, and it is a measure of electrical efficiency. Basically, if the energy efficiency of a process is high, its E_{EO} will be low [32].

Considering the first-order degradation kinetics, the UV dose for each process can be calculated using Eq. (17) [32,73]. E_{EO} is obtained from the inverse of the slope of the plot of log (C_0/C) versus energy dose (kWh/m^3) [32]:

$$\text{UV Dose} = \frac{1{,}000 \times \text{lamp power}\,(\text{kW}) \times \text{time}\,(\text{h})}{\text{treated volume}\,(\text{L})} \quad (17)$$

The total operating cost of the photocatalytic degradation of the 2,4-D herbicide at optimum conditions was calculated using Eqs. (18) and (19). Economic analysis was carried out to determine the operating cost of the photocatalytic treatment of the 2,4-D herbicide in a batch reactor under different conditions such as UV/TiO_2 and UV/TiO_2/H_2O_2. The COD removal was below average under the working conditions involving

the sole use of UV and for conditions involving the sole use of TiO_2. Using the experimental results, the operating cost of each kilogram (kg) of COD removal from the 2,4-D herbicide in wastewater was calculated in terms of US Dollars (USD) and Turkish Lira (TRY) by using Eqs. (3.7) and (3.8) [75]. In both equations, energy consumption is the sum of the energy requirement of the magnetic stirrer (8 W only for stirring), the UV lamp (36 W), the peristaltic pump (30 W), and the air pump (3 W).

$$\text{Total consumed energy}\left(\text{kWh}\right)=\frac{\text{Consumed power}\left(\text{W}\right)\times\text{Reaction time}\left(\text{dk}\right)}{\left(1{,}000\times 60\right)} \tag{18}$$

$$\text{Total operating cost}\left(\frac{\text{USD}}{\text{kg}}\right)=\frac{\text{Total consumed energy}\left(\text{kWh}\right)\times\text{Unit energy cost}\left(\text{USD}/\text{kWh}\right)}{\left(C_{\text{initial COD}}-C_{\text{final COD}}\right)\left(\frac{\text{mg}}{L}\right)\times\text{Treated volume}\left(V\right)}\times 10^{6}\left(\frac{\text{mg}}{\text{kg}}\right) \tag{19}$$

E_{EO} values revealed that the electrical efficiency in the photocatalysis of 25 mgL^{-1} of 2,4-D was better in the UV/TiO_2/H_2O_2 system (Table S1).

Economic analysis was performed under different working conditions to evaluate the operating cost of the photocatalytic treatment of the 2,4-D herbicide: for example, UV/TiO_2 and UV/TiO_2/H_2O_2 in batch mode. The COD removal was below average only in the UV process, and the process involving the sole use of TiO_2. The degradation half-lives calculated – based on Eq. (13) – were 15.71 and 29.12 min^{-1} for 25 and 50 mg L^{-1}, respectively. The estimated power input to the system was 77 W. The energy requirements for the degradation of half of the initial amounts were 20.30 Wh (e.g., 0.073 MJ) for 25 mg L^{-1} and 37.61 Wh (e.g., 0.135 MJ) for 50 mg L^{-1}.

According to Table S2, the photocatalytic process with UV/TiO_2/H_2O_2 – compared to the treatment process with UV/TiO_2 – had a rapid potential that exhibited a higher percentage of organic matter removal. Economic analysis is necessary to evaluate the cost effectiveness of a treatment process [77]. In their study, Aye et al. [47] reported that, in the absence of H_2O_2, a textile wastewater treatment of 47% removal was obtained after the decolorization process in a period three times longer than the illumination period in the presence of H_2O_2. In this study, using H_2O_2 as a subsidiary to the reaction in the photocatalytic system resulted in the removal of a significant amount of COD in a period as short as 150 min (from 65.52% with the UV/TiO_2 process to 85.19% with the UV/TiO_2/H_2O_2 process). According to Table S2, cost reduction is a function of the optimum time required for achieving maximum removal efficiency [75]. In addition to reactor geometry and hydrodynamic resistance time, it is a process that requires taking the deactivation of the photocatalyst into consideration for technical applications [38].

4. Conclusion

UVA/TiO_2 photocatalysis with the addition of H_2O_2 is more effective than UVA/TiO_2 photocatalysis without H_2O_2 (using TiO_2 + UVA + H_2O_2) with the addition of an optimum 150 mg L^{-1} of H_2O_2. The 2,4-D degradation rate decreased with the increase in initial 2,4-D concentration. The pseudo-first-order kinetic model fitted the experimental data well, and the photocatalytic degradation process was explained by the modified L–H model. The k_c and K_{LH} values were determined to be 1.293 mg L^{-1} min^{-1} and 0.232 L mg^{-1}, respectively. The UVA/TiO_2/H_2O_2 process was more effective under a batch photocatalytic process in terms of low cost and higher efficiency per kg of COD removal from wastewater. The study is significant in terms of the application of UVA/TiO_2/H_2O_2 photocatalysis as a pretreatment for 2,4-D herbicide wastewater at a pH of 5 for a biological treatment.

Acknowledgments

This study was financially supported by AIBU Scientific Research Projects, Project Number: 2016.09.02.1032. The authors would like to thank TUBITAK for the Ph.D. Dissertation Grant given to Gamze Dogdu Okcu within the 2211/A National Doctoral Scholarship Program.

Symbols

C	—	2,4-D concentration at time t, mg L^{-1}
C_0	—	initial 2,4-D concentration, mg L^{-1}
E_{EO}	—	electrical energy per order, k Wh m^{-3} order^{-1}
K	—	Langmuir adsorption constant
k_{app}	—	apparent kinetic constant, min^{-1}
K_{LH}	—	Langmuir–Hinshelwood adsorption equilibrium constant, L mg^{-1}
k_r	—	reaction rate constant, g mg^{-1} min^{-1}
L–H	—	Langmuir–Hinshelwood
P	—	UV lamp power, kW
r_0	—	initial degradation rate, mg L^{-1} dk^{-1}
R^2	—	linear regression coefficient
$t_{1/2}$	—	half-life reaction time, minutes
V	—	treated volume, L
θ	—	fraction of catalyst surface covered

References

[1] M.A. Oturan, J.J. Aaron, Advanced oxidation processes in water/wastewater treatment: principles and applications. A review, Crit. Rev. Environ. Sci. Technol., 44 (2014) 2577–2641.

[2] M.A. Vishnuganth, R. Neelancherry, M. Kumar, N. Selvaraju, Carbofuran removal in continuous-photocatalytic reactor: Reactor optimization, rate-constant determination and carbofuran degradation pathway analysis, J. Environ. Sci. Health. Part B., 52 (2017) 353–360.

[3] R.K. Singh, L. Philip, S. Ramanujam, Removal of 2,4-dichlorophenoxyacetic acid in aqueous solution by pulsed corona discharge treatment: Effect of different water constituents, degradation pathway and toxicity assay, Chemosphere, 184 (2017) 207–214.

[4] C. Berberidou, V. Kitsiou, E. Kazala, D.A. Lambropoulou, A. Kouras, C.I. Kosma, T.A. Albanis, I. Poulios, Study of the decomposition and detoxification of the herbicide bentazon by heterogeneous photocatalysis: Kinetics, intermediates and transformation pathways, Appl. Catal. B., 200 (2017) 150–163.

[5] Turkish Republic Official Gazette Turkish Regulation on Human Consumption Water, Part Four, Appendix-1, Chemical Parameters (25730), 17.02.2005, 19.

[6] United States Prevention Agency (EPA), Prevention, Pesticides and Toxic Substances (7508C). Reregistration Eligibility Decision for 2,4-d, (2005), https://archive.epa.gov/pesticides/reregistration/web/pdf/24d_red.pdf (accessed 10 November 2017).

[7] C.A. Sandoval-Carrasco, D. Ahuatzi-Chacón, J. Galíndez-Mayer, N. Ruiz-Ordaz, C. Juárez-Ramírez, F. Martínez-Jerónimo, Biodegradation of a mixture of the herbicides ametryn, and 2,4-D, chlorophenoxyacetic acid (2,4-D) in a compartmentalized biofilm reactor, Bioresour. Technol., 145 (2013) 33–36.

[8] Y. Ordaz-Guillén, C.J. Galíndez Mayer, N. Ruiz-Ordaz, C. Juárez-Ramírez, F. Santoyo-Tepole, O. Ramos-Monray, Evaluating the degradation of the herbicides picloram and 2,4-D in a compartmentalized reactive biobarrier with internal liquid recirculation, Environ. Sci. Pollut. Res., 21 (2014) 8765–8773.

[9] K. Park, J. Park, J. Kim, I.S. Kwak, Biological and molecular responses of *Chironomus riparius* (Diptera, Chironomidae) to herbicide 2,4-D (2,4-dichlorophenoxyacetic acid), Comp Biochem Physiol C Toxicol Pharmacol., 151 (2010) 439–446.

[10] X. Quan, J. Ma, W. Xiong, X. Wang, Bioaugmentation of half-matured granular sludge with special microbial culture promoted establishment of 2,4-dichlorophenoxyacetic acid degrading aerobic granules, Bioprocess Biosyst. Eng., 38 (2015) 1081–1090.

[11] K. Li, J.-Q. Wu, L.-L. Jiang, L.-Z. Shen, J.-Y. Li, Z.-H. He, P. Wei, Z. Lv, M.-F. He, Developmental toxicity of 2,4-dichlorophenoxyacetic acid in zebrafish embryos, Chemosphere., 171 (2017) 40–48.

[12] S. Mekonen, R. Argaw, A. Simanesew, M. Houbraken, D. Senaeve, A. Ambelu, P. Spanoghe, Chemosphere pesticide residues in drinking water and associated risk to consumers in Ethiopia, Chemosphere, 162 (2016) 252–260.

[13] B.M. Teklu, P.I. Adriaanse, M.M.S. Ter Horst, J.W. Deneer, P.J. Van den Brink, Surface water risk assessment of pesticides in Ethiopia, Sci. Total Environ., 508 (2015) 566–574.

[14] US EPA, Health advisory: 2,4-Dichlorophenoxyacetic acid. Environmental Protection Agency, Washington, DC, (1987), https://www.epa.gov/sites/production/files/2015-06/documents/ny_hh_367_w_03121998.pdf. (accessed on 26 August 2018).

[15] USEPA, Ground water and drinking water regulation, (2017), https://www.epa.gov/groundwater-and-drinking-water/national-primary-drinking-water-regulations. (accessed on 15 May 2017).

[16] N.L. Finčur, J.B. Krstić, F.S. Šibul, D.V. Šojić, V.N. Despotović, N.D. Banić, J.R. Agbaba, B.F. Abramović, Removal of alprazolam from aqueous solutions by heterogeneous photocatalysis: Influencing factors, intermediates, and products, Chem. Eng. J., 307 (2017) 1105–1115.

[17] N.A. Laoufi, F. Bentahar, Pesticide removal from water suspension by UV/TiO_2 process: a parametric study, Desal. Water Treat., 52 (2014) 1947–1955.

[18] A.C. Affam, M. Chaudhuri, Degradation of pesticides chlorpyrifos, cypermethrin and chlorothalonil in aqueous solution by TiO_2 photocatalysis, J. Environ. Manage., 130 (2013) 160–165.

[19] M. Qamar, M. Muneer, Comparative photocatalytic study of two selected pesticide derivatives, indole-3-acetic acid and indole-3-butyric acid in aqueous suspensions of titanium dioxide, J. Hazard. Mater., B120 (2005) 219–227.

[20] M. Yeber, E. Paul, C. Soto, Chemical and biological treatments to clean oily wastewater: optimization of the photocatalytic process using experimental design, Desal. Water Treat., 47 (2012) 295–299.

[21] M.N. Chong, Y.J. Cho, P.E. Poh, B. Jin, Evaluation of Titanium dioxide photocatalytic technology for the treatment of reactive Black 5 dye in synthetic and real greywater effluents, J Clean Prod., 89 (2015) 196–202.

[22] D.E. Santiago, J.M. Doña-Rodríguez, J. Araña, C. Fernández-Rodríguez, O. González-Díaz, J. Pérez-Peña, A.M.T. Silva, Optimization of the degradation of imazalil by photocatalysis: Comparison between commercial and lab-made photocatalysts, Appl. Catal. B., 138–139 (2013) 391–400.

[23] S.K. Deokar, S.A. Mandavgane, Rice husk ash for fast removal of 2,4-dichlorophenoxyacetic acid from aqueous solution, Adsorp. Sci. Technol., 33 (2015) 429–440.

[24] T. Lee, S. Kurata, C. Nakatsu, Y. Kamagata, Molecular analysis of bacterial community based on 16S rDNA and functional genes in activated sludge enriched with 2,4-dichlorophenoxyacetic acid (2,4-D) under different cultural conditions, Microb Ecol., 49 (2015) 151–162.

[25] N.S. Trivedi, R.A. Kharkar, S.A. Mandavgane, Utilization of cotton plant ash and char for removal of 2, 4-dichlorophenoxyacetic acid, Resource-Eff Technol., 2 (2016) 39–46.

[26] L.O. Conte, A.V. Schenone, O.M. Alfano, Photo-Fenton degradation of the herbicide 2,4-D in aqueous medium at pH conditions close to neutrality, J. Environ. Manage., 170 (2016) 60–69.

[27] M. Thrills, J. Petal, X. Domènech, Redox photodegradation of 2,4-dichlorophenoxyacetic acid over TiO_2, Appl. Catal. B., 5 (1995) 377–387.

[28] H.K Singh, M. Muneer, Photodegradation of a herbicide derivative, 2,4-dichlorophenoxy acetic acid in aqueous suspensions of titanium dioxide, Res Chem Intermediate., 30 (2004) 317–329.

[29] K. Djebbar, A. Zertal, T. Sehili, Photocatalytic degradation of 2,4-dichlorophenoxyacetic acid and 4-chloro-2-methylphenoxyacetic acid in water by using TiO_2, Environ. Technol., 27 (2006) 1191–1197.

[30] S. Kundu, A. Pal, A.K. Dikshit, UV ınduced degradation of herbicide 2,4-D: kinetics, mechanism and effect of various conditions on the degradation, Sep. Purif. Technol., 44 (2005) 121–129.

[31] I. Talinli, G.K. Anderson, Interference of hydrogen peroxide on the standard COD test, Water Res., 26 (1992) 107–110.

[32] N. Daneshvar, D. Salari, A. Niaei, A.R. Khataee, Photocataytic degradation of the herbicide erioglaucine in the presence of nanosized titanium dioxide: comparison and modeling of reaction kinetics, J. Environ. Sci. Health., Part B., 41 (2006) 1273–1290.

[33] H. Zúňiga-Benitez, C. Aristizábal-Ciro, G.A. Peñuela, Heterogeneous photocatalytic degradation of the endocrine-disturbing chemical benzophenone-3: Parameters optimization and by-products identification, J. Environ. Manage., 167 (2016) 246–258.

[34] E. Bazrafshan, F.K. Mostafapour, H. Faridi, M. Farzadkia, S. Shahnaz, A. Sohrabi, Removal of 2,4-dichlorophenoxyacetic acid (2,4-D) from aqueous environments using single-walled carbon nanotubes, Health Scope., 1 (2013) 39–46.

[35] C.H. Yu, C.H. Wu, T.H. Ho, P.K.A. Hong, Decolorization of C.I. Reactive Black 5 in UV/TiO_2, UV/oxidant and UV/TiO_2/oxidant systems: A comparative study, Chem. Eng. J., 158 (2010) 578–583.

[36] S. Bouafia-Chergui, H. Zemmouri, M. Chabani, A. Bensmaili, TiO_2-photocatalyzes degradation of tetracycline: kinetic study,

adsorption isotherms, mineralization and toxicity reduction, Desal. Water Treat., 57 (2016) 16670–16677.
[37] K.H. Oh, O. Tuovinen, Bacterial degradation of phenoxy herbicide mixtures 2,4-D and MCPP, Bull. Environ. Contam. Toxicol., 47 (1991) 222–229.
[38] M. Woche, N. Scheibe, W. von Tümpling, M. Schwidder, Degradation of the antiviral drug zanamivir in wastewater-The potential of a photocatalytic treatment process, Chem. Eng. J., 287 (2016) 674–679.
[39] L. Khenniche, L. Favier, A. Bouzaza, F. Fourcade, F. Aissani, A. Amrane, Photocataytic degradation of bezacryl yellow in batch reactors - feasibility of the combination of photocatalysis and a biological treatment, Environ. Technol., 36 (2015) 1–10.
[40] A. Piscopo, D. Robert, J.V. Weber, Influence of pH and chloride anion on the photocatalytic degradation of organic compounds: Part I. Effect on the benzamide and para-hydroxybenzoic acid in TiO_2 aqueous solution, Appl. Catal. B., 35 (2001) 117–124.
[41] S.J. Jafari, G. Moussavi, H. Hossaini, Degradation and mineralization of diazinon pesticide in UVC and UVC/TiO_2 process, Desal. Water Treat., 57 (2016) 3782–3790.
[42] R. Rajeswari, S. Kanmani, A study on degradation of pesticide wastewater by TiO_2 photocatalysis, J. Sci. Ind. Res., 68 (2009) 1063–1067.
[43] L. Yahia Cherif, I. Yahiaoui, F. Aissani-Benissad, K. Madi, N. Benmehdi, F. Fourcade, A. Amrane, Heat attachment method for the immobilization of TiO_2 on glass plates: application to photodegradation of basic yellow dye and optimization of operating parameters, using response surface methodology, Ind. Eng. Chem. Res., 53 (2014) 3813–3819.
[44] T.J. Kaur, A.P. Toor, R. Wanchoo, UV-assisted degradation of propiconazole in a TiO_2 aqueous suspension: identification of transformation products and the reaction pathway using GC/MS, Int. J. Environ. Anal. Chem., 95 (2015) 494–507.
[45] E.S. Elmolla, M. Chaudhuri, Photocatalytic degradation of amoxicillin, ampicillin and cloxacillin antibiotics in aqueous solution using UV/TiO_2 and UV/H_2O_2/TiO_2 photocatalysis, Desalination, 252 (2010) 46–52.
[46] M.G. Alalm, A. Tawfik, S. Ookawara, Comparison of solar TiO_2 photocatalysis and solar photo-Fenton for treatment of pesticides industry wastewater: Operational conditions, kinetics, and costs, J. Water Process Eng., 8 (2015) 55–63.
[47] T. Aye, W.A. Anderson, M. Mehrvar, Photocatalytic treatment of cibacron brilliant yellow 3G-P (reactive yellow 2 textile dye), J. Environ. Sci. Health., Part A., 38 (2003) 1903–1914.
[48] N. Daneshvar, M.J. Hejazi, B. Rangarangy, A.R. Khataee, Photocatalytic degradation of an organophosphorus pesticide phosalone in aqueous suspensions of titanium dioxide, J. Environ. Sci. Health., Part B., B39 (2004) 285–296.
[49] L.-A. Lu, Y.-S. Ma, M. Kumar, J.-G. Lin, Photo-Fenton pre-treatment of carbofuran-analyses via experimental design, detoxification and biodegradability enhancement, Sep. Purif. Technol., 81 (2011) 325–331.
[50] H. Dong, G. Zeng, L. Tang, C. Fan, C. Zhang, X. He, Y. He, An overview on limitations of TiO_2-based particles for photocatalytic degradation of organic pollutants and the corresponding countermeasures, Water Res., 1 (2015) 128–46.
[51] A. Amalraj, A. Pius, Photocatalytic degradation of monocrotophos and chlorpyrifos in aqueous solution using TiO_2 and UV irradiation, J. Water Process Eng., 7 (2015) 94–101.
[52] A. Verma, N.T. Prakash, A.P. Toor, Photocatalytic degradation of herbicide isoproturon in TiO_2 aqueous suspensions: study of reaction ıntermediates and degradation pathways, Environ Technol., 33 (2013) 402–409.
[53] E. Diaz, M. Cebrian, A. Bahamonde, M. Faraldos, A.F. Mohedano, J.A. Casas, J.J. Rodriguez, Degradation of organochlorinated pollutants in water by catalytic hydrodechlorination and photocatalysis, Catal. Today, 266 (2016) 168–174.
[54] S. Yahiat, F. Fourcade, S. Brosillon, A. Amrane, Photocatalysis as a pre-treatment prior to a biological degradation of cyproconazole, Desalination, 281 (2011) 61–67.
[55] E. Deletze, A. Antoniadis, V. Kitsiou, E. Kostoppulou, D. Lutic, I. Cretescu, I. Poulios, Photocatalytic treatment of colored wastewater from medical laboratories: photo-degradation of nuclear fast red, Desal. Water Treat., 57 (2016) 18897–18905.
[56] J.C. D'Oliveira, C. Minero, E. Pelizzetti, P. Pichat, Photodegradation of dichlorophenols and trichlorophenols in TiO_2 aqueous suspensions: kinetic effects of the positions of the Cl atoms and identification of the intermediates, J. Photochem. Photobiol., A., 72 (1993) 26–267.
[57] B. Huang, C. Lei, C. Wei, G. Zeng, Chlorinated volatile organic compounds (Lc-VOCs) in environment-sources, potential human health impacts, and current remediation technologies, Environ. Int., 71 (2014) 118–138.
[58] E.C. Catalkaya, F. Kargi, Dehalogenation, degradation and mineralization of diuron by peroxone (peroxide/ozone) treatment, J Environ Sci Health A., 44 (2009) 630–638.
[59] A.T. Nguyen, C.T. Hsieh, R.S. Juang, Substituent effects on photodegradation of phenols in binary mixtures by hybrid H_2O_2 and TiO_2 suspensions under UV irradiation, J Taiwan Inst Chem Eng., 62 (2016) 68–75.
[60] I. Pavlovic, C. Barriga, M.C. Hermosin, J. Cornejo, M.A. Ulibarri, Adsorption of acidic pesticides 2,4-D, clopyralid and picloram on calcined hydrotalcite, Appl. Clay Sci., 30 (2005) 125–133.
[61] D.L. Pavia, G.M. Lampman, G.S. Kriz, J.R. Vyvyan, Introduction to Spectroscopy, 4th ed., Brooks Cole Cengage Learning, USA, 2008.
[62] K. Thamaphat, P. Limsuwan, B. Ngotawornchai, Phase characterization of TiO_2 powder by XRD and TEM, Kasetsart J. Nat. Sci., 42 (2008) 357–361.
[63] T. Phonkhokkong, T. Thongtem, S. Thongtem, A. Phuruangrat, W. Promnopas, Synthesis and characterization of TiO_2 nanopowders for fabrication of dye sensitized solar cells, Dig. J. Nanomater Biostruct., 11 (2016) 81–90.
[64] D. Bamba, P. Atheba, D. Robert, A. Trokourey, B. Dongui, Photocatalytic degradation of the diuron pesticide, Environ. Chem. Lett., 6 (2008) 163–167.
[65] S. Khezrianjoo, H.D. Revanasiddappa, Langmuir–Hinshelwood kinetic expression for the photocatalytic degradation of metanil yellow aqueous solutions by ZnO catalyst, Chem. Sci. J., 2012 (2012) CSJ-85.
[66] J.A. Bergendahl, T.P. Thies, Fenton's oxidation of MTBE with zerovalent ıron, Water Res., 38 (2004) 327–334.
[67] Al-Ekabi, N. Serpone, Kinetics studies in heterogeneous photocatalysis. I. Photo-catalytic degradation of chlorinated phenols in aerated aqueous solutions over titania sup-ported on a glass matrix, J. Phys. Chem., 92 (1988) 5726–5731.
[68] R.W. Matthews, Environment: Photochemical and Photocatalytic Processes. Degradation of Organic Compounds, E. Pelizzetti, M. Schiavello Eds., Photochemical Conversion and Storage of Solar Energy, Springer, Dordrecht, 1991, Doi: https://doi.org/10.1007/978-94-011-3396-8_22.
[69] C.G. da Silva, J.L. Faria, Photochemical and photocatalytic degradation of an azo dye in aqueous solution by UV irradiation, J. Photochem. Photobiol., A., 155 (2003) 133–143.
[70] S.P. Kamble, S.B. Sawant, V.G. Pangarkar, Photocatalytic mineralization of phenoxyacetic acid using concentrated solar radiation and titanium dioxide in slurry photo-reactor, Chem. Eng. Res. Des., 84 (2006) 355–362.
[71] P. Nitoi, I. Oancea, L. Cristea, L.A. Constantin, G. Nechifor, Kinetics and mechanism of chlorinated aniline degradation by TiO_2 photocatalysis, J. Photochem. Photobiol., A., 298 (2015) 17–23.
[72] J.R. Bolton, M.I. Stefan, Fundamental photochemical approach tı the concepts of fluence (UV dose) and electrical energy efficiency in photochemical degradation reactions, Res Chem Intermediate., 28 (2002) 857–870.
[73] J.R. Bolton, K.G. Bircher, W. Tumas, C.A. Tolman, Figures-of-merit for the technical development and application of advanced oxidation technology for both electric-and solar-driven systems (IUPAC Technical Report), Pure Appl. Chem., 73 (2001) 627–637.
[74] J.C. Cardoso, G.G. Bessegato, M.V.B. Zanoni, Efficiency comparison of ozonation, photolysis, photocatalysis and photoelectrocatalysis methods in real textile wastewater decolorization, Water Res., 98 (2016) 39–46.

[75] C.R. Asha, M.A. Vishnuganth, N. Remya, N. Selvaraju, M. Kumar, Livestock wastewater treatment in batch and continuous photocatalytic systems: performance and economic analyses, Water Air Soil Pollut., 226 (2015) 132.
[76] N. Azbar, T. Yonar, K. Kestioglu, Comparison of various advanced oxidation processes and chemical treatment methods for COD and color removal from a polyester and acetate fiber dyeing effluent, Chemosphere, 55 (2004) 35–43.
[77] N. Remya, J.G. Lin, Current status of microwave application in wastewater treatment-A review, Chem. Eng. J., 166 (2011) 797–813.

Supplementary Information

Appendix I

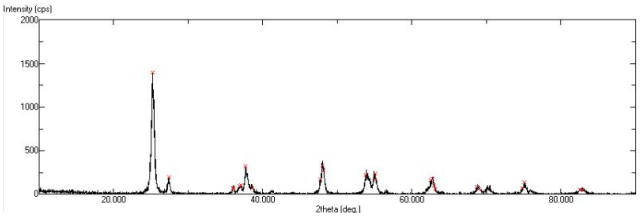

Fig. S1. X-ray diffraction of P25 TiO_2 nanopowder in anatase phase.

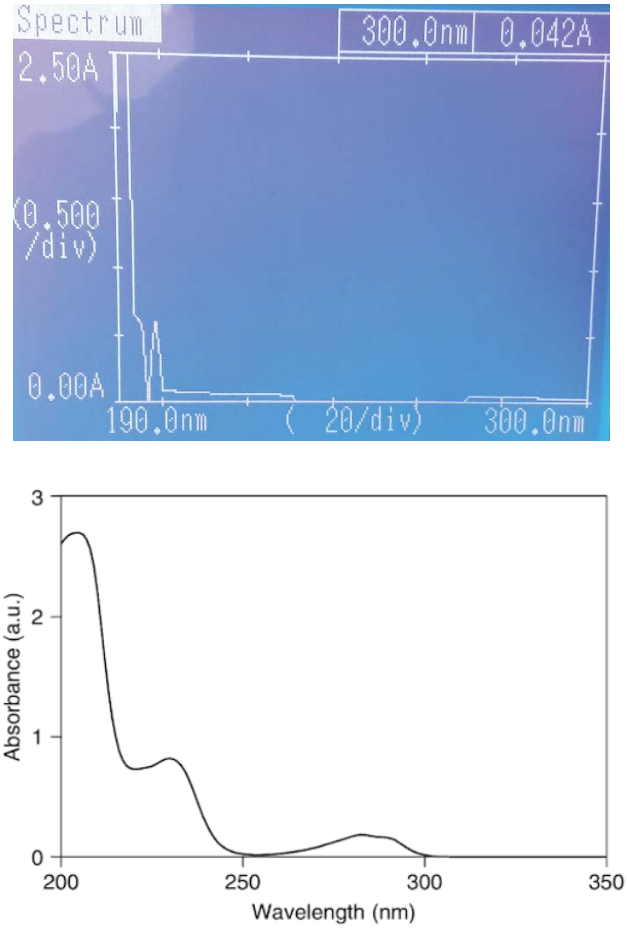

Fig. S2. UV spectrum of 2,4-D (20 mg L^{-1}).

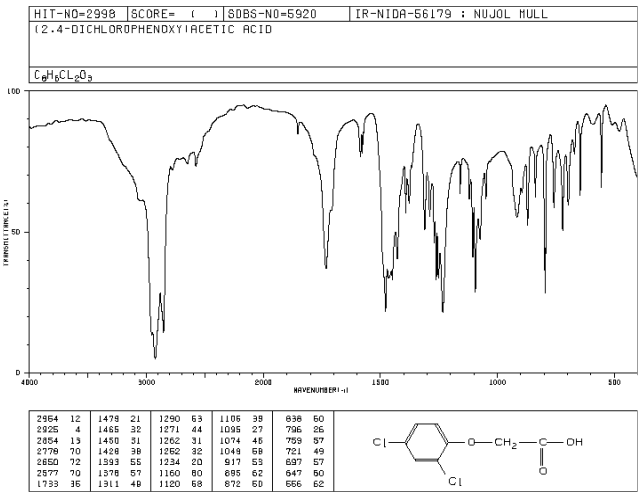

Fig. S3. FTIR spectrum of the original 2,4-D herbicide.

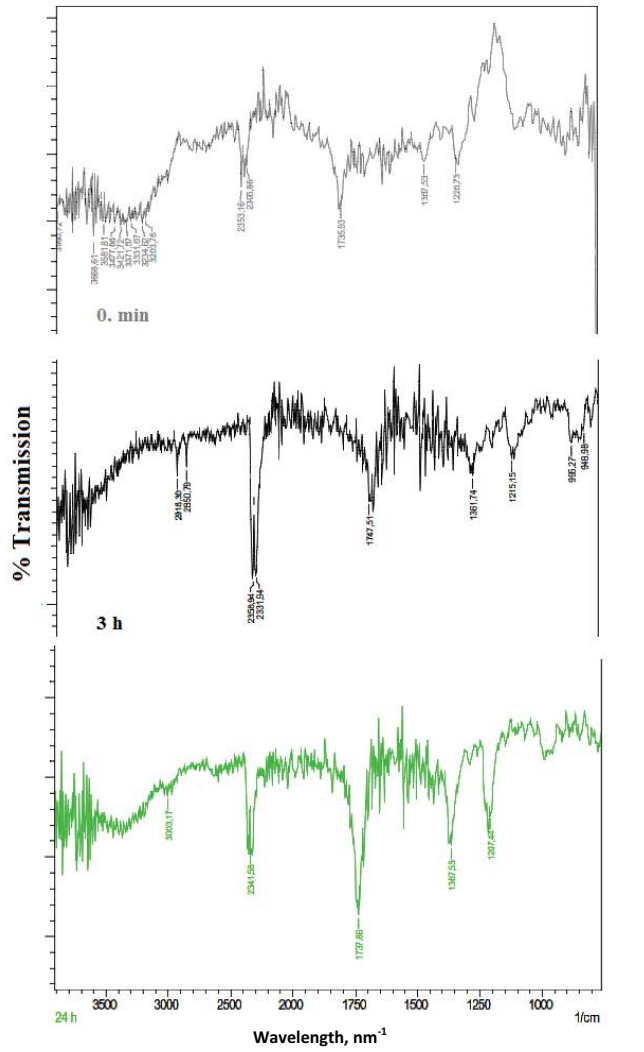

Fig. S4. FTIR spectrum of the 2,4-D herbicide (a) before photocatalysis (0 min), (b) 3 h after photocatalysis, and (c) 24 h after photocatalysis.

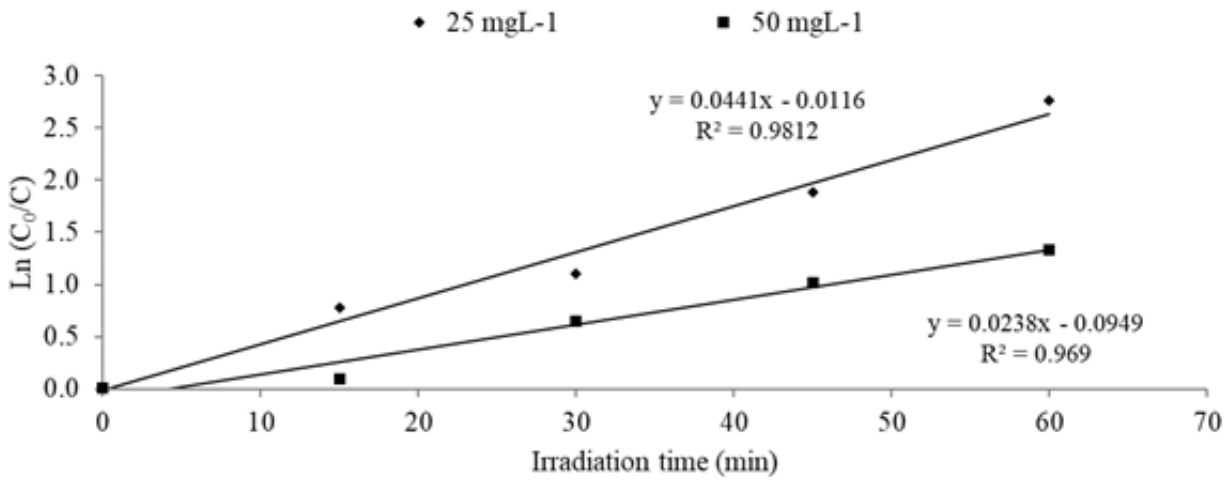

Fig. S5. The linear change in ln (C_0/C) versus time for the photocatalytic degradation of 2,4-D at different initial concentrations.

Table S1
The effect of the initial 2,4-D herbicide concentration on kinetic constant, regression coefficient, and electrical energy per order (E_{EO}).

Experimental conditions				
Initial concentration (mg L^{-1})	TiO_2 concentration (mg L^{-1})	H_2O_2 concentration (mg L^{-1})	pH	E_{EO} (k Wh m^{-3} $order^{-1}$)
25	1.5	–	5	33,333
25	1.5	150	5	125,000
50	1.5	–	5	50,000

Table S2
The cost analysis for 2,4-D herbicide removal in the photoreactor under two different sets of working conditions.

	2,4-D conc. (mg L^{-1})	TiO_2 conc. (mg L^{-1})	TiO_2 costs (USD/g)	H_2O_2 conc. (mg L^{-1})	H_2O_2 costs (USD/L)	pH	COD removal (mg L^{-1})	Reaction time (min)	Total power consumed per mg 2,4-D removal (k Wh)	Total cost (USD/kg)	Total cost (TRY/kg)
UV/TiO_2	25	1.5	1.89	–	28.15	5	10.5	15	0.0194	219.909	785.432
	50	1.5	1.89	–	28.15	5	38	180	0.2325	723.864	2579.17
$UV/TiO_2/H_2O_2$	25	1.5	1.89	150	28.15	5	55	15	0.0194	71.662	157.577
	50	1.5	1.89	150	28.15	5	122.5	150	0.1938	216.721	673.889

1. UV radiation intensity is the same in all systems (36 W). 2. The working volume of the reactor is 1 L. 3. Total energy consumption (P) 77 W (energy consumption by the electronic magnetic stirrer (8 W), air pump (3 W), peristaltic pump (30 W), and UV lamp (36 W) 4. Unit power cost 0.42 TL/kWh and 11.8 US cents/kWh) [TEDAŞ, 2017 July] 5. TiO_2 price for 100 G:160.50 EUR (Sigma-Aldrich©) 6. H_2O_2 (30 %) price for 1 L: 23.90 EUR. * Consumed per each mg of 2,4-D removal